

# ROOM TEMPERATURE FERROMAGNETISM IN Co-DOPED ZnO NANOPARTICLES: MILLING TIME DEPENDENCE AND ANNEALING EFFECT

BAPPADITYA PAL\* and P. K. GIRI†

*Department of Physics and Centre for Nanotechnology  
Indian Institute of Technology Guwahati, Guwahati-781039, India*

\**bpal@iitg.ernet.in*

†*giri@iitg.ernet.in*

We report on the occurrence of room temperature ferromagnetism in Co-doped ZnO nanoparticles (NPs). Doping is performed by ball milling of 3 wt% of Co mixed with ZnO nanopowders (commercial) for durations of 2–8 h. X-ray diffraction data and high-resolution transmission electron microscopy (HRTEM) confirm the absence of metallic Co clusters or any other phase different from wurtzite-type ZnO. The magnetization ( $M$ – $H$  curve) measured at room temperature exhibited the clear ferromagnetic characteristic with saturation magnetization ( $M_s$ ) and coercive field ( $H_c$ ) of the order of 3–4 emu/g and 225 Oe, respectively. Post-growth annealing at 250°C results in an increase of  $M_s$  by a small magnitude, while annealing at 500°C results in reduction of  $M_s$ . UV–visible absorption spectra show small redshift in the absorption peaks in the Co-doped ZnO NPs due to the incorporation of Co atoms in ZnO lattice. Room temperature photoluminescence studies show enhanced near-band-edge emission at 378 nm in the doped NPs as compared to the undoped NPs indicating negligible presence of defects in the doped ZnO crystals. Contribution of intrinsic defects and magnetic impurities in the observed ferromagnetism is discussed.

*Keywords:* ZnO; dilute magnetic semiconductors; ferromagnetism; ball milling.

## 1. Introduction

Transition metal doped ZnO is a promising candidate material for the field of spintronics.<sup>1</sup> Spin–electronics (or spintronics) is based on concepts that utilize the quantum mechanical spin properties of carriers in addition to the carrier charge in realizing electronic functionality providing both enhanced performance and new functionalities in traditional microelectronic devices.<sup>2–4</sup> Dietl *et al.*<sup>5</sup> predicted the existence of high-temperature ferromagnetism (FM) in some magnetically doped wide bandgap  $p$ -type semiconductors that has led to multiple experimental and computational studies of these materials. Particularly, transition-metal-doped ZnO DMSs have been extensively investigated since theoretical studies predicted its Curie temperature ( $T_c$ ) to be above room

temperature.<sup>6</sup> Moreover, ZnO is an interesting direct wide bandgap (3.27 eV) semiconductor being explored for numerous applications in optoelectronics.<sup>7</sup>

However, experimental observations about the nature of the magnetic properties of Co-doped ZnO synthesized by different methods are controversial for both thin films and bulk samples.<sup>8</sup> Conflicting results have been reported in the case of Co-doped ZnO<sup>9</sup> but recently room temperature FM in single-phase Co-doped<sup>10,11</sup> and Mn-doped<sup>12</sup> ZnO have been reported. Earlier works are mostly performed through thin film preparation using different techniques like magnetron sputtering unit, pulsed laser deposition, etc.

In this work, we report on the magnetic and structural properties of Co-doped ZnO NPs synthesized by the ball-milling method. X-ray diffraction (XRD) and

transmission electron microscopy (TEM) are used to examine phase segregation. UV–visible optical absorption and photoluminescence (PL) measurements are used to infer the substitution of Co inside the Zn lattice. Vibrating sample magnetometer (VSM) is employed to measure the magnetic properties. The observed magnetization and hysteresis behavior are discussed with reference to the role of defects, free carriers, and doping in the ZnO sublattice.

## 2. Experimental Details

The starting materials were commercial ZnO nanopowder (purity 99.999%, Sigma Aldrich) and metallic cobalt (Co) powder (99.5%, Loba Chemie). Co powder used was 3% of the weight of ZnO nanopowder. The mixed powder was milled in a mechanical ball-milling machine (Retsch, PM 100) at 300 rpm for a duration of 2 h, 5 h, and 8 h in a Zirconium oxide vial under atmospheric pressure and temperature. Zirconium oxide balls were used to avoid contamination. The ball to powder mixture weight ratio was taken as 10:1. Sample milled for 5 h was post-annealed at two different temperatures: 250°C and 500°C for 5 h. The crystal structures were characterized by XRD (Bruker D8 Advance, with, Cu  $K_{\alpha}$  radiation). Morphology and structures were observed by high-resolution transmission electron microscopy (HRTEM) (JEOL-JEM 2010, 200 keV). HRTEM imaging and microanalysis by energy-dispersive X-ray spectroscopy (EDS) were conducted in the same microscope. The magnetic properties of the samples were measured by using a Lakeshore (7410) vibrating sample magnetometer (VSM). The UV–visible spectroscopy measurements were recorded using a commercial spectrophotometer (Varian) with a monochromated Xenon lamp source. The steady-state photoluminescence (PL) spectrum was recorded at room temperature by using a 325 nm He–Cd laser excitation coupled in a commercial high-end fluorimeter (Edinburg, FSP920).

## 3. Results and Discussion

### 3.1. Structural characterization

Figure 1 shows some typical powder XRD patterns of the ZnCoO NPs. All the observed diffraction peaks can be indexed to a ZnO wurtzite structure, and no other impurity phase was found, which indicates that the Co ion successfully occupies the lattice site rather than interstitial ones. Compared

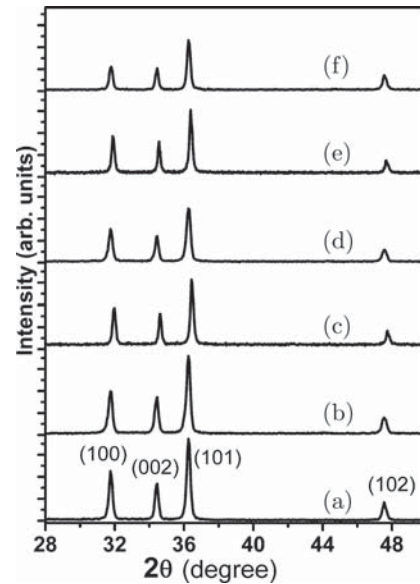


Fig. 1. XRD patterns of the Co-doped ZnO samples for different milling times: (a) undoped ZnO (b) 2 h, (c) 5 h, (d) 8 h milled Co-ZnO. XRD pattern of 5 h milled samples annealed at (e) 250°C, (f) 500°C.

to undoped ZnO, the doped samples show lowering of intensity and increase in full width at half maxima (FWHM). Average particle size calculated from XRD peak is about 50 nm for undoped sample which goes down to 40 nm for the milled samples. Due to the introduction of Co atoms in the ZnO lattice, there may be lattice strain associated with the doping and as a result a decrease in intensity and higher FWHM is expected in as-doped ZnCoO NPs. However, we cannot exclude the possibility of formation of other precipitates or clusters small enough not to be detected in conventional XRD measurement.

Figure 2(a) shows low-magnification TEM images of the Co-doped ZnO NPs prepared after 5 h of milling. The micrograph reveals particle size distribution with the length and breadth of the particles ranging from 40 to 100 nm. HRTEM images are presented in Fig. 2(b), which shows that all the nanoparticles are single crystalline and free from any major lattice defects. The  $d$ -spacing of the crystal plane is calculated as 0.246 nm, which shows the preferable crystal growth plane is (101). The selected area diffraction (SAD) patterns shown in Fig. 2(c) confirms that the ZnCoO NPs are single crystals. All the  $d$ -spacings calculated from the SAD pattern are close to ZnO. It clearly indicates the nanoparticles are single crystalline in nature and in the wurtzite phase. There are no cobalt clusters

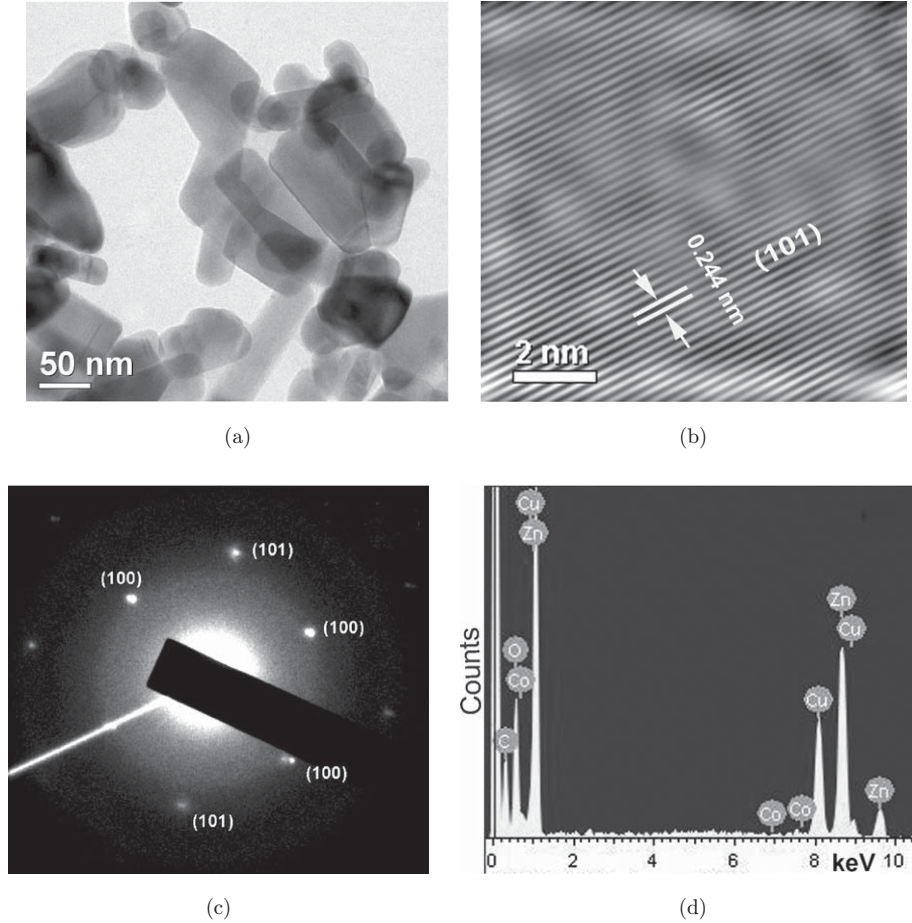


Fig. 2. HRTEM images of: (a) Co-doped ZnO NPs, (b) lattice of doped NPs showing no clustering of Co, (c) corresponding SAED pattern, (d) EDS spectra showing Co in ZnO NPs.

observed in the as-prepared sample particles. The EDS spectra measured on few single particles at the nm scale show Zn, Co, and O related peaks, as shown in Fig. 2(c), besides Cu and C peaks from carbon-coated Cu grid used in TEM, which indicate that cobalt ions were uniformly distributed in the entire ZnCoO samples.

### 3.2. Magnetic characterization

The ferromagnetic behavior at room temperature is studied in the Co-doped ZnO samples. No trace of FM was observed in the undoped sample. Figure 3 shows the ( $M-H$ ) loops measured at 300 K for different hours milled and annealed samples treated at 250°C and 500°C. The saturation magnetizations ( $M_s$ ) of the samples increase from 3.40 emu/g for 2 h milled sample to 4.14 emu/g for 8 h milled sample.  $M_s$  increases with the milling time possibly due to increase in electrons which induce more effective ferromagnetic couplings between doped

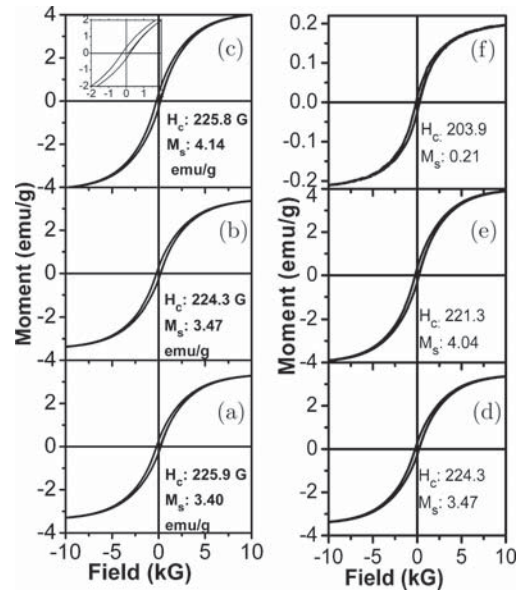


Fig. 3.  $M-H$  loop showing hysteresis of the Co-doped ZnO: (a) 2 h; (b) 5 h; (c) 8 h milled. The inset shows the magnified  $M-H$  loop. Hysteresis of 5 h milled sample annealed at (e) 250°C, (f) 500°C in air.

Co<sup>2+</sup> ions. Post-growth air annealing affects the magnetization; initially  $M_s$  increases to 4.04 emu/g for 250°C annealing and then decreases to a low value of 0.21 emu/g for annealing at 500°C while the coercivity ( $H_c$ ) remains almost unchanged (225–200 Oe). The ferromagnetism observed in Co-doped ZnO nanocrystals could arise from a number of possible sources: as carrier-mediated exchange mechanism, Co precipitation, and the formation of CoO. However, CoO phase can be easily ruled out, since CoO is antiferromagnetic with a Neel temperature of 293 K. Second, metallic Co is also an unlikely source of this ferromagnetism, as XRD and HRTEM results clearly show no metallic Co clusters in the NPs. UV–visible absorption, photoluminescence (PL) spectra showed a bandgap shift which suggests Co<sup>2+</sup> ions were successfully incorporated into the wurtzite lattice at the Zn<sup>2+</sup> sites. Thus, ferromagnetism in the Co-doped ZnO NPs could be considered as a result of the exchange interaction between free delocalized carriers (hole or electron) and the localized  $d$  spins on the Co<sup>2+</sup> ions. Native point defects such as O vacancy and Zn interstitial are very common in ZnO and they are likely to contribute to the observed ferromagnetism in the ZnCoO nanocrystals. However, defect contribution is expected to be insignificant in the present case, as we have seen improved PL emission in the Co-doped NPs.

### 3.3. Optical absorption and photoluminescence studies

Many groups have confirmed that Co automatically substitutes on Zn sites using optical methods such as XPS and optical absorption.<sup>13,14</sup> The fourfold coordinated ionic radii of Co<sup>2+</sup> (0.058 nm) and Zn<sup>2+</sup> (0.06 nm) are very similar and result in a large solubility of Co<sup>2+</sup> in the ZnO lattice.<sup>15</sup> The UV–visible spectrum at room temperature was used primarily to verify the bandgap shift shown in Fig. 4(a). A small redshift is observed in the bandgap energy for the Co-doped samples compared to the undoped ZnO. The redshift is typically attributed to the  $sp$ – $d$  exchange between the ZnO band electrons and localized  $d$ -electrons associated with the doped Co<sup>2+</sup> cations. The interaction leads to corrections in the energy bands: the conduction band is lowered and the valence band is raised causing the bandgap to shrink. Figure 4(b) shows the PL spectra at room temperature. Two distinct peaks are observed from the undoped and doped samples: peak at  $\sim$ 376 nm is due to near-band edge emission (NBE)

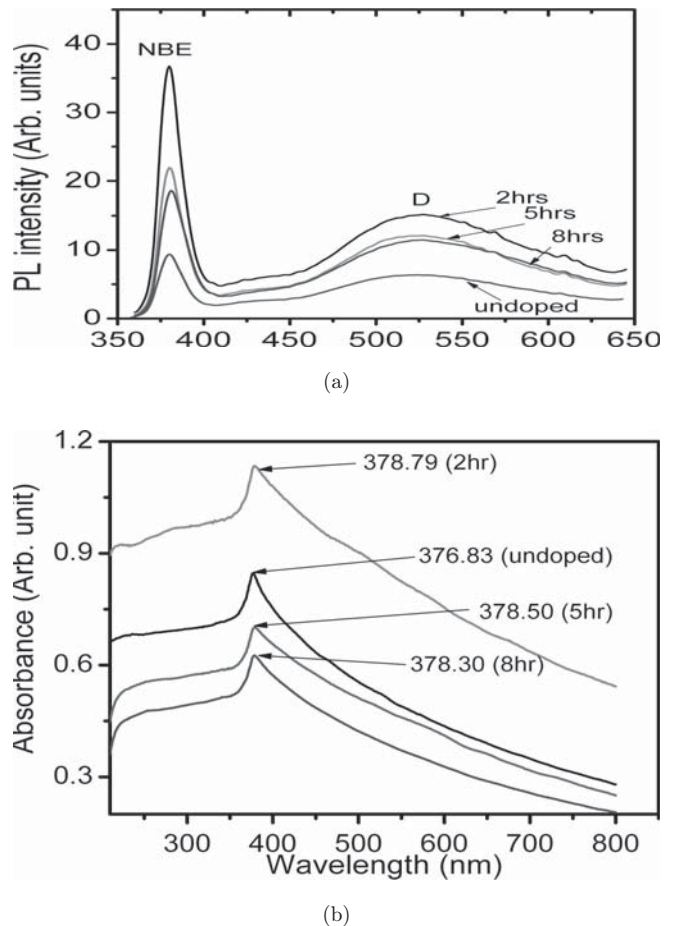


Fig. 4. UV–visible absorption spectra of undoped and Co-doped ZnO NPs. (b) RT PL spectra of undoped and Co-doped ZnO NPs. Improved PL is observed in 2 h milled (doped) ZnO NPs.

and peak at  $\sim$ 525 nm is due to the intrinsic defect-related band ( $D$ ). Note that NBE emission band does not show any significant shift after 2 h of milling but it shows a large increase in the intensity with respect to the undoped ZnO NPs. This improved PL emission indicates that the doped samples have fewer defects to play any significant role in the observed FM behavior at room temperature.

## 4. Conclusion

In summary, nanocrystalline ZnCoO has been synthesized by a simple ball-milling method. Microstructure analysis shows that the nanoparticles are of single crystalline ZnO wurtzite structure. XRD, HRTEM, EDS, UV–visible, and PL measurements indicate that Co<sup>2+</sup> substitute into ZnO lattice at Zn<sup>2+</sup> site, instead of forming impurity compound or cobalt oxide. The exchange interactions between Co<sup>2+</sup> ions mediated by carriers contribute to the

ferromagnetism at room temperature. Our work further shows that defects do not play any significant role in the observed FM in ZnCoO. Here, RT FM have been obtained in Co-doped ZnO DMS material and its Curie temperature ( $T_c$ ) is predicted to be above room temperature. So it will be an important material for the development of semiconductors that can retain their FM properties above room temperature for the realization of practical commercial devices.

## References

1. S. J. Pearton *et al.*, *Mater. Sci. Eng. R.* **40**, 137 (2003).
2. S. J. Pearton, D. P. Norton, R. Frazier, S. Y. Han, C. R. Abernathy and J. M. Zavada, *IEEE Proc. Circuits Devices Syst.* **152**, 312 (2005).
3. S. D. Sarma, *Nat. Matters* **2**, 292 (2003).
4. S. J. Pearton, C. R. Abernathy, M. E. Overberg, G. T. Thaler, A. F. Hebard, Y. D. Park, F. Ren, J. Kim and L. A. Boatner, *J. Appl. Phys.* **1**, 93 (2003).
5. T. Dietl, H. Ohno *et al.*, *Science* **287**, 1019 (2000).
6. K. Sato and H. Katayama-Yosida, *Semicond. Sci. Technol.* **17**, 357 (2002).
7. S. J. Pearton, D. P. Norton, K. Ip, Y. W. Heo and T. Steiner, *Superlatt. Microstruct.* **34**, 3 (2003).
8. T. Fukumura *et al.*, *Appl. Surf. Sci.* **223**, 62 (2004).
9. S. W. Jung, S. J. An, G. C. Yi, C. U. Jung, S. I. Lee and S. Cho, *Appl. Phys. Lett.* **80**, 4561 (2002).
10. L. Yan, C. K. Ong and X. S. Rao, *J. Appl. Phys.* **96**, 508 (2004).
11. S. Ramachandran, A. Tiwari and J. Narayan, *Appl. Phys. Lett.* **84**, 5255 (2004).
12. P. Sharma *et al.*, *Nat. Mater.* **2**, 673 (2003).
13. A. C. Tuan *et al.*, *Phys. Rev. B* **70**, 054424 (2004).
14. K. Samanta *et al.*, *Appl. Phys. Lett.* **87**, 101903 (2005).
15. Z. Jin *et al.*, *Cryst. Growth* **214**, 215 (2000).